ADVANCED BIOSYSTEMS

www.adv-biosys.com

Capturing the Onset of Bacterial Pulmonary Infection in Acini-On-Chips

Arbel Artzy-Schnirman, Hikaia Zidan, Shani Elias-Kirma, Lee Ben-Porat, Janna Tenenbaum-Katan, Patrick Carius, Ramy Fishler, Nicole Schneider-Daum, Claus-Michael Lehr, and Josué Sznitman*

Bacterial invasion of the respiratory system leads to complex immune responses. In the deep alveolar regions, the first line of defense includes foremost the alveolar epithelium, the surfactant-rich liquid lining, and alveolar macrophages. Typical in vitro models come short of mimicking the complexity of the airway environment in the onset of airway infection; amongst other, they neither capture the relevant anatomical features nor the physiological flows innate of the acinar milieu. Here, novel microfluidic-based acini-on-chips that mimic more closely the native acinar airways at true scale with an anatomically inspired, multigeneration alveolated tree are presented and an inhalation-like maneuver is delivered. Composed of human alveolar epithelial lentivirus immortalized cells and macrophages-like human THP-1 cells at an air–liquid interface, the models maintain critically an epithelial barrier with immune function. To demonstrate, the usability and versatility of the in vitro platforms, a realistic inhalation exposure assay mimicking bacterial infection is recapitulated, whereby the alveolar epithelium is exposed to lipopolysaccharides droplets directly aerosolized and the innate immune response is assessed by monitoring the secretion of IL8 cytokines. These efforts underscore the potential to deliver advanced in vitro biosystems that can provide new insights into drug screening as well as acute and subacute toxicity assays.

1. Introduction

Lung inflammation plays a critical role in many respiratory diseases including acute respiratory distress syndrome (ARDS), chronic obstructive pulmonary disease (COPD), asthma, and cystic fibrosis (CF) amongst others.[1] Traditionally, the immunological mechanisms underlying such conditions have been studied using animal models and/or in vitro models. While animal models of lung inflammation remain an invaluable tool for both basic research and preclinical trials, their use is known to be limited by the underlying differences between such in vivo models and the human body.[2–4] Concurrently, in vitro models,[5] most commonly consisting of submerged cell cultures seeded in well plates or grown on transmembrane well inserts, are not only limited in their ability to faithfully recapitulate critical biological functions of the innate organ, they also lack essential phenotypes that range from anatomical traits to physiological flows and mechanical stresses applied in vivo. To overcome the aforementioned shortcomings, there is a growing need for alternative in vitro platforms that better mimic the pulmonary milieu.[6]

In the last decade microfluidics, and so-called organ-on-chips in particular, have gained significant momentum in laying the foundations for constructing advanced in vitro models that can mimic more faithfully physiologically relevant organ functions. This includes, for example, the critical role played by (air and blood) flows in the respiratory zone (i.e., pulmonary acinus). Multiple groups have leveraged lung-on-chip models to recreate breathing phenomena; yet, the bulk of such efforts has relied on single channels or isolated airsacs,[7–9] thereby neglecting important anatomical features of the deep lung environment that lead to acinar-specific aerosol deposition outcomes and may play a significant role in drug distribution.[10] A faithful reconstitution of the underlying lung architecture, and in particular the intricate foam-like structure of deep alveolated airways, remains technically challenging and is still widely beyond reach.[6] Although the aforementioned studies as well as others represent major advances in investigating alveolar

A. Artzy-Schnirman, H. Zidan, S. Elias-Kirma, L. Ben-Porat, J. Tenenbaum-Katan, R. Fishler, J. Sznitman
Department of Biomedical Engineering
Technion-Israel Institute of Technology
Haifa, Israel
E-mail: sznitman@bm.technion.ac.il
P. Carius, N. Schneider-Daum, C.-M. Lehr
Helmholtz Institute for Pharmaceutical Research Saarland (HIPS)
Helmholtz Center for Infection Research (HZI)
Saarland University
66123 Saarbrücken, Germany
P. Carius, C.-M. Lehr
Biopharmaceutics and Pharmaceutical Technology
Department of Pharmacy
Saarland University
66123 Saarbrücken, Germany
The ORCID identification number(s) for the author(s) of this article can be found under https://doi.org/10.1002/adbi.201900026.

DOI: 10.1002/adbi.201900026

physiology,[7,8,11–14] they come short in both mimicking accurately the morphology and ensuring respiratory airflow distributions pertinent to acinar airways in vivo.[6,15] This latter aspect is critical when considering that by and large in vitro inhalation exposure assays on airway barriers have relied on instilling liquid suspensions directly onto cell cultures. More recent efforts have pushed to deliver aerosols via direct spraying,[16–18] yet there is still a gap in capturing physically realistic aerosol transport at an ALI in mimicking more truthfully the fate of aerosols depositing on the airway lumen.

Beyond the anatomical and physiological flow determinants of the acinar regions, three main cell types line the lumen of the deep lungs in vivo. These include alveolar epithelial cells type 1 (AT1) that enable gas exchange and barrier function, alveolar epithelial cells type 2 (AT2) responsible for surfactant-secretion, and alveolar macrophages that orchestrate the innate immune response at the barrier site. AT2 cells also serve as progenitor cells, maintaining the regenerative capacity of the alveolar sacs and alveolar macrophages. Importantly, epithelial cells together with alveolar macrophages are known to have immunomodulatory functions characterized by the secretion of proinflammatory cytokines.[19,20] To date, the majority of microfluidic-based in vitro alveolar models have advocated the use of primary pulmonary cells. While it is generally accepted that primary alveolar cells directly isolated from human lungs better preserve physiological properties of the lung tissue, ongoing hurdles include difficulties in obtaining such cells and the huge variability between donors, in addition to the challenges of cell culturing alone.[21,22] Most significantly, benchmarking standardized assays with primary cells is critically challenging whereas past cell lines do not hold sufficient. In circumventing such challenges, a novel alternative and highly relevant epithelial model was recently developed, i.e., human alveolar epithelial lentivirus immortalized (hAELVi) cells. Briefly, hAELVi cells feature AT1-like phenotypes corresponding to the normal composition of the alveolar epithelium.[23] Furthermore, they maintain critical epithelial barrier functions leading to high transepithelial electrical resistance (TEER), in analogy to primary cells harvested from human tissue.[21] Such characteristics render them most suitable for drug delivery and cytotoxicity assays amongst others but have never been leveraged beyond traditional in vitro assays.

Here, we have developed a novel anatomically inspired acini-on-chip platform that mimics more closely native acinar airways at true scale in a multigeneration alveolated tree. Together with hAELVi cells and a model for human monocyte derived macrophages, differentiated to macrophage-like cells at an ALI, our in vitro devices underline the reconstitution of a functional alveolar barrier including immune functions. To model alveolar macrophages, we use the THP-1 cell line; a cell line that has been extensively used[23,24] to study monocyte and macrophage functions, signaling pathways, and drug transport among others. In addition, it is an established cell line to induce pro-inflammatory activation of lung epithelial cells.[25] As a proof-of-concept of the model's potential, we recapitulate in vitro an aerosol exposure assay and monitor the proinflammatory response of the alveolar epithelial barrier. To model inflammatory events typically going along with bacterial infections we used lipopolysaccharide (LPS), a notorious stimulator of the innate immune system and constituting a major outer surface membrane protein expressed on Gram-negative bacteria,[26] i.e., in mycobacterium tuberculosis. The reconstituted alveolar epithelium in coculture with the macrophages is exposed to LPS-laden aerosols via a realistic inhalation-like exposure composed of airborne droplets under airflow, whereby ensuing cell response is assessed by monitoring IL8 secretion. Overall, our versatile model captures anatomical and physiological characteristics while preserving essential functions of the homeostatic cellular microenvironment. Such platform represents an important milestone toward the realization of new in vitro tools that could better predict clinical outcomes.

2. Results and Discussion

2.1. Acini-On-Chip Establishment

To assess the biological applicability of our acini-on-chip biosystems, two anatomically inspired microfluidic devices of increasing complexity were designed. First, a microfluidic device featuring an anatomically inspired, multigeneration alveolated airway tree was established (**Figure 1**a). The device consists of six asymmetric dichotomously branching generations, where saccular airspaces, corresponding to early stages during pulmonary development, are mimicked by enlarged cavities at the distal generations (see Figure 1a, blue arrows). Underalveolated branches, on the other hand, are depicted by cavity depletions off from the proximal ducts (see Figure 1a, red arrows). To adequately capture the acinar length scales of developing acinar airways, our designs feature characteristic channels of 170 µm width by 100 µm height with alveolar diameters of 155 µm, following morphometric data from lung casts.[27,28] As the measured data are acquired in fully inflated lungs representative of total lung capacity, our acinar airway anatomies are scaled to match lung volumes corresponding to functional residual capacity (FRC) in line with respiratory volumes representative of tidal breathing. The selected FRC values are matched to pediatric populations exhibiting height and weight distributions as obtained from lung cast measurements.[29] A notable feature of our microfluidic design is given in the matched flow rates at the distal ends of the acinar tree (see Figure 1a, stars); such requirement stems from the in vivo environment, where no slip flow conditions on the alveolar walls assure zero flow across all terminal ends of the acinus.[15] Here, we have established an analogous condition by adjusting the pathways between each terminal end of the microfluidic tree and the common outlet. This ensures matching the same pressure drop across all paths by having channels of equal length within the microfluidic-based in vitro device.

The acinar airway tree model (Figure 1a) offers an anatomically relevant model that demonstrates the versatility of microfluidic-based lung models in realizing intricate morphologies of the developing deep airways. Concurrently, it poses technical difficulties in achieving full epithelial coverage due to the vast surface area combined with such intricate length scales and morphological features (e.g., bifurcations, alveoli, etc.). In parallel, we thus opted for an anatomically simpler, alveolated airway model based on a recent design useful for investigating

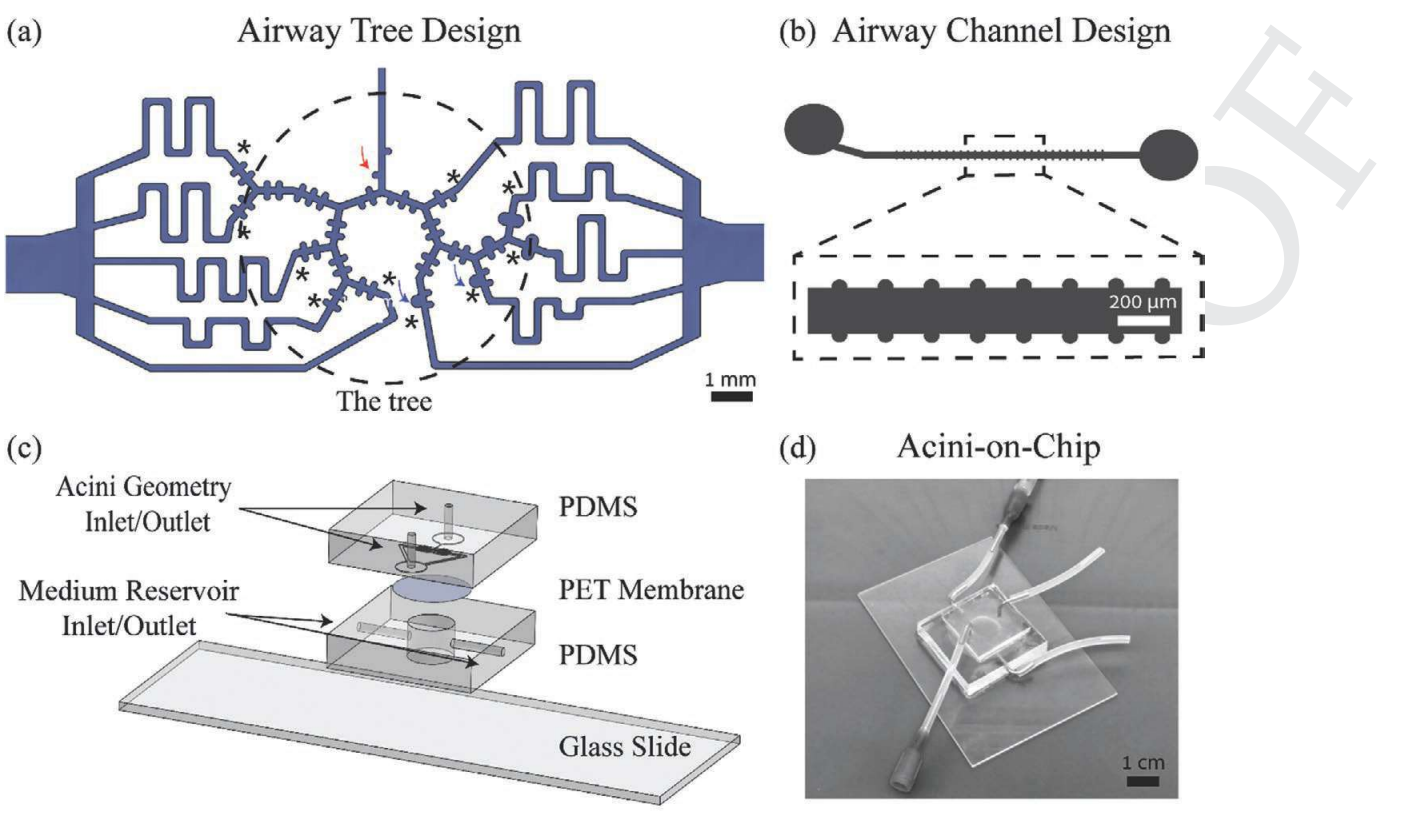

Figure 1. Anatomically inspired microfluidic model of acinar airways. a) Microfluidic alveolated acini-on-chip design featuring a multigeneration asymmetrically bifurcating model of subacinar airway structures. Distal airways are modeled by saccular alveoli (blue arrows) and underpopulated air-ducts (red arrows). Note that the model provides equal flow at each terminal end, by adjusting and matching the length of a channel connecting the common microfluidic outlet and the last generation of our acinar tree. b) A microfluidic device combining straight ducts (resembling airways) lined with cylindrical cavities (mimicking alveolar spaces). c) Exploded view of the computer-aided drawing (CAD) of the acini-on-chip. A compartmentalized sandwich structure is assembled on a glass slide, and a porous membrane is positioned between the PDMS alveolated airway tree (apical side) and a bottom reservoir (basal side) to perfuse culture media (with integrated openings for inlet and outlet). On the apical side, two openings (inlet and outlet) allowing selective insertion of desired components to the upper tree, e.g., cells for seeding followed by airflow to reproduce physiological flow conditions. d) Snapshot of the assembled acini-on-chip.

barrier functions[30] (Figure 1b). This design mimics underlying features of the acinar ducts only. The microfluidic model combines straight channels of 166 µm width and 100 µm height, regularly lined with cylindrical cavities of 40 µm radius. The alveolar opening angle ($\alpha = 60°$) was selected to match closely that frequently used to model fully developed adult alveoli.[31]

To render our microfluidic acinar designs compatible for cell culture and thereby recapitulate underlying characteristics of the alveolar epithelial barrier at an ALI, devices were assembled by integrating the poly(dimethylsiloxane) (PDMS) polymer microfluidic channels (on the apical side) to a PDMS pool containing cell medium (on the basal side), separated by a 10 µm thick porous polyester (PET) membrane (Dow Corning) with 0.4 µm pore sizes (see Figure 1c). These so-called microfluidic "sandwich" structures, namely device assemblies featuring an ALI separated by an epithelial barrier with medium perfusion from the basal side, have been increasingly utilized in recent years.[6,8,32] Finally, tubing is connected to the apical and basal compartments, respectively, to allow easy access of fluid and/or airflow at the hands of the end user (Figure 1d).

2.2. Epithelial Barrier Characteristics

A growing number of cell lines derived from different regions of the airways are available for in vitro studies of the respiratory environment.[33] To date, the most commonly used and widely characterized cell type to model the alveolar epithelium remains the A549 (American Type Culture Collection, ATCC CL-185) cell line; an epithelial model immortalized and derived from human lung adenocarcinoma.[34] The morphology and biochemical features of this cell line resemble the characteristics of human alveolar type 2 cells in situ. A major limitation of the A549 cells remains their inability to form functional intercellular tight junctions, resulting in so-called "leaky" monolayers of the epithelium; a major limitation in realizing attractive in vitro models for drug permeability and absorption assays. In the past few years, alveolar primary cells have become more commonly used to overcome the limitations of A549 cells.[11,35–38] Nevertheless, the limited number of cells that can be received during each isolation, the short life span and the uncertainty due to donor variation represent important drawbacks.[39] Here, we present acini-on-chip cultured with hAELVi cells (**Figure 2**). Unlike primary cells, hAELVi cells can be cultured up to passage 75, under liquid–liquid as well as ALI conditions. Furthermore, and in contrast to A549 cells, hAELVi cells resemble AT1 cells and maintain their capacity to form tight intercellular junctions, with high transepithelial electrical resistance (>1000 Ω cm^2).[23]

To the best of our knowledge, the present acini-on-chip constitutes the first use of hAELVi cells as an in vitro functional biosystem of the alveolar epithelial barrier. Namely, the epithelial barrier was established by coating the device's membranes with type I collagen and fibronectin solution. Following

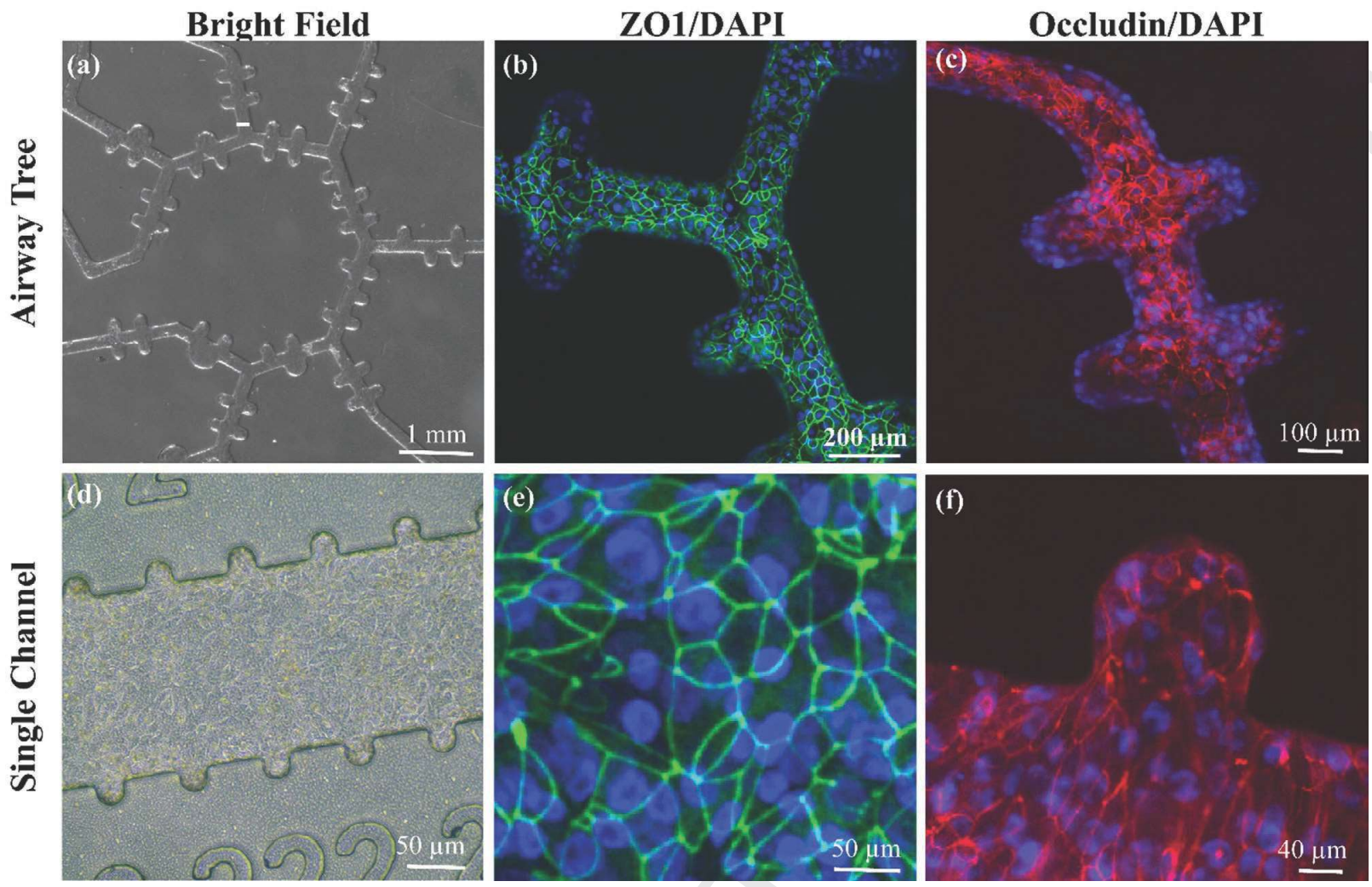

Figure 2. Anatomically inspired microfluidic models of alveolated airways seeded with hAELVi cells in the full alveolated airway tree (top row) and acinar ducts (bottom row). a,d) Brightfield image. b,e) Immunofluorescence micrographic views of hAELVi cells immunolabeled with anti-ZO-1 (green) and DAPI (blue) at (a) day 17, and (b) day 18 cultivated at an ALI from day 2. c,f) Immunofluorescence micrographic views of hAELVi cells immunolabeled with antioccludin (red) DAPI (blue).

coating, hAELVi cells were seeded in the apical compartment and allowed to adhere under liquid–liquid conditions. To mimic in vivo conditions, medium was removed after 48 h from the apical compartment and cells were allowed to grow at the ALI for at least 12 days. At that time point, a densely packed monolayer of cells can be observed under light microscopy (see Figure 2a,d). To confirm the formation of tight junctions, the expression of two characteristic proteins were examined: zona occludens (ZO-1) and occludin. Clearly labeled tight junction complexes appeared as a continuous thin line between adjacent cells in both the alveolated tree (Figure 2b,c) and the airway channel design (Figure 2e,f), similar to those observed on traditional Transwell inserts (see Figure S1, Supporting Information).

To recapitulate relevant immune functions of the acinar environment with alveolar macrophages, THP-1 monocytes were differentiated into macrophage-like cells. Differentiated THP-1 cells were then trypsinized and seeded on top of preformed hAELVi monolayer and the devices were further cultivated for up to 7 days. In each experiment, two sets of devices were seeded simultaneously; cocultures of hAELVi cells and THP-1 macrophage-like cells and monocultures of hAELVi cells, for direct comparison. The differentiation of THP-1 cells into macrophage-like cells was determined by using antihuman CD11b antibody, which stains macrophages[40] (**Figure 3**a,b). Notably, TEER measurements were used to evaluate the integrity of the epithelial monolayer and have thus become a standard experimental method. Here as a control, each passage of hAELVi cells, seeded in a device, was also seeded on an insert and TEER was monitored over time (see Figure S2, Supporting Information) to ensure the capability of each specific cell passage to deliver a functional barrier, with values reaching well within 1000 Ω cm^2. In the acini-on-chip platforms, however, TEER measurements are still challenging as no practical and validated approach has yet been developed.[41] The minute dimensions of the channels together with the stringent requirement for a closed and controlled environment to support cell growth creates limited access to the epithelial layer leading to difficulties in measuring adequately TEER.

To circumvent such challenges, we have evaluated the barrier properties of the coculture using a hydrophilic molecule, i.e., sodium fluorescein (FluNa). This follows as high TEER correlates with low transepithelial transport and provides a viable alternative to TEER measurements.[23] Briefly, FluNa was added to the apical compartment and a transport buffer was introduced to the basolateral compartment. At different time points, 30 µL samples were taken from the basolateral compartment and the volume lost during sampling was replaced with fresh buffer. The sodium fluorescein amount in the samples was measured and the apparent permeability (P_{app}) was calculated

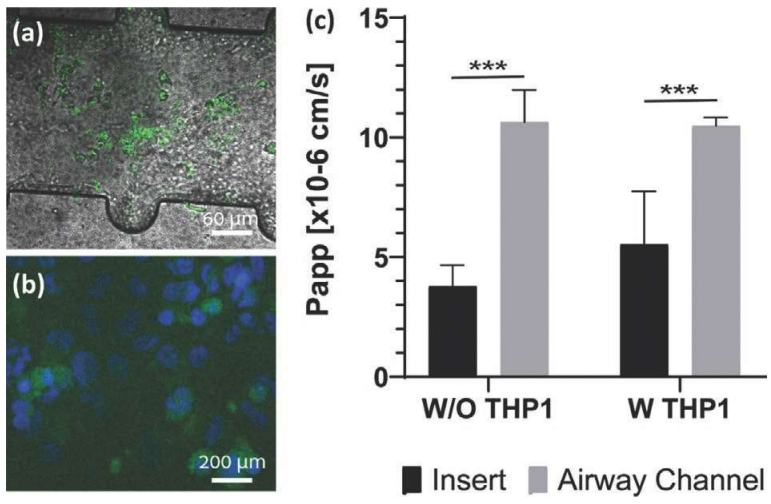

Figure 3. Morphology and barrier properties of hAELVi/THP-1 cocultures. a) Airway channel seeded with coculture of hAELVi (day 21) cells and THP-1 (day 7), overlaying of bright field image and on THP-1 cells stained with anti-CD11b antibody (Green). b) Immunofluorescence micrographic views of THP-1 cultured on-chip for 7 days at the ALI, stained with anti-CD11b antibody (green) and DAPI (blue). c) Transport of FluNa across a monolayer of hAELVi. The THP-1 cells were seeded between day 17 and 20 on a preformed hAELVi monolayer on insert and devices. Data shown as mean ± SD (insert: W-THP-1 with $n = 8$, WO-THP-1 with $n = 4$, airway channel W-THP-1 with $n = 7$, and WO-THP-1 with $n = 4$) $^{***}p < 0.001$.

following Elbert et al.[22] To compare between the different culturing conditions in the device and the traditional insert, cells were grown until a full confluent monolayer was achieved (i.e., 14–35 days) to allow the formation of tight junctions. At that time point, differentiated THP-1 cells were seeded respectively in the Transwell inserts and the microfluidic devices, and the transport assay was performed after 72 h following a previous protocol reported by Kletting et al.[40] on inserts. As can be seen in Figure 3c, no statistical differences were found in P_{app} measurements between the airway channels and the Transwell inserts; both in the absence or presence of THP-1 cells (i.e., mono- vs cocultures). Indeed, measured P_{app} yields values within the same order of magnitude, as previously highlighted for hAELVi cells monolayer specifically,[23] although transepithelial transport is slightly higher within the microfluidic device compared to the Transwell insert. We hypothesize that the main reason for such discrepancy may arise due to the interface between the PET membrane and the channel walls made of PDMS since the cells grow only on the membrane but FluNa may nevertheless translocate across the interface between the two materials (PET and PDMS).

As a final remark in considering epithelial barrier characteristics, we open here a short parenthesis in evaluating the benefits of both advocated platforms, i.e., the complex acinar airway network (Figure 1a) compared with straight alveolated channels (Figure 1b). As presented in Figure 2, a functional epithelial barrier is established across the full airway tree that carefully adheres to the geometrical constraints of the underlying substrate. Yet, it has been recently shown that a mere 0.4% lack in epithelial coverage of the surface leads to an 80% decrease in TEER measurements,[42] correlating with high P_{app} values. With this in mind, guaranteeing a strict 100% surface coverage across the intrinsically complex airway network featuring a large number of bifurcations, branches, and alveolar cavities is not realistic. Thus, we have introduced a device platform (i.e., acinar ducts) that delivers a compromise in anatomical complexity (i.e., straight channels) while still offering relevant anatomical features of the acinus (i.e., alveoli). Together, our two complementary platforms offer benefits for different applications depending on the specific endpoints. While in both devices functional tight junctions are formed (Figure 2b,e), if the scope of the in vitro assay is targeted at pure transport assays, the simpler device anatomy would be preferential as guaranteed by P_{app} values (Figure 3).

2.3. Aerosol Inflammation Exposure Assay

In the alveolar regions, the first line of defense includes the alveolar epithelium, the surfactant-rich alveolar fluid lining and the alveolar macrophages. AT1 and AT2 are known to have immunomodulatory functions characterized by the secretion of proinflammatory cytokines.[19] AT1 contain toll-like receptor 4 (TLR4), i.e., a receptor for LPS, a cell wall protein found on Gram-negative bacteria. LPS is a strong stimulator of the innate arm of the immune system, which is known to cause acute lung injury in vivo[43] and has been widely used to simulate bacterial infections in vitro.[44] Notably, LPS stimulation of alveolar epithelial cells and macrophages has been shown to produce proinflammatory cytokines. As a proof-of-concept of the potential and suitability of our in vitro platforms for various aerosol exposure assays, our acini-on-chip were exposed to nebulized aerosols. While inhalation therapies often aim at tracheobronchial delivery in the context of asthma and obstructive diseases (e.g., COPD), delivering therapeutics to the deeper pulmonary alveolar regions has drawn increased attention in recent years with potential applications for systemic delivery[45,46] (e.g., vaccinations[47,48] and insulin delivery[49]) as well as antibiotics for targeted treatments of pulmonary infections,[50] such as in pneumonia and CF. Our in vitro biosystems lend themselves as a potent alternative for conducting early-stage, preclinical studies in assessing inhalation therapies.

To induce an inflammatory response, the acini-on-chips were directly connected to a standard mini compressor nebulizer. All chips were exposed to nebulized aerosols for up to 4 min, with phosphate buffered saline (PBS) as the carrier liquid (i.e., deposition field inside device, **Figure 4**a). 48 h after the exposure assay, the medium from the basal compartment was collected and analyzed for IL8 secretion using an enzyme-linked immunosorbent assay (ELISA). IL8 plays a role in the pathogenesis of various diseases, including ARDS and asthma. IL8 has a major role in neutrophil chemoattractant and activating, one of the major immune cell types that accumulate in the airway when inflamed. As can be seen in Figure 4b, IL8 secretion levels were higher upon LPS exposure in both the airway channel and tree for hAELVi cells alone, thereby supporting the role played by the epithelial monolayer itself. The IL-8 levels of the co- and monocultures with nebulized PBS show similar values as exposing the samples to PBS without the nebulizer (data not shown), representing the basal secretion levels. Coculturing of hAELVi cells with THP-1 macrophage-like cells (Figure 4c) resulted in a similar yet enhanced trend in secretion, i.e., IL-8 levels were higher compared to the control in both models. As

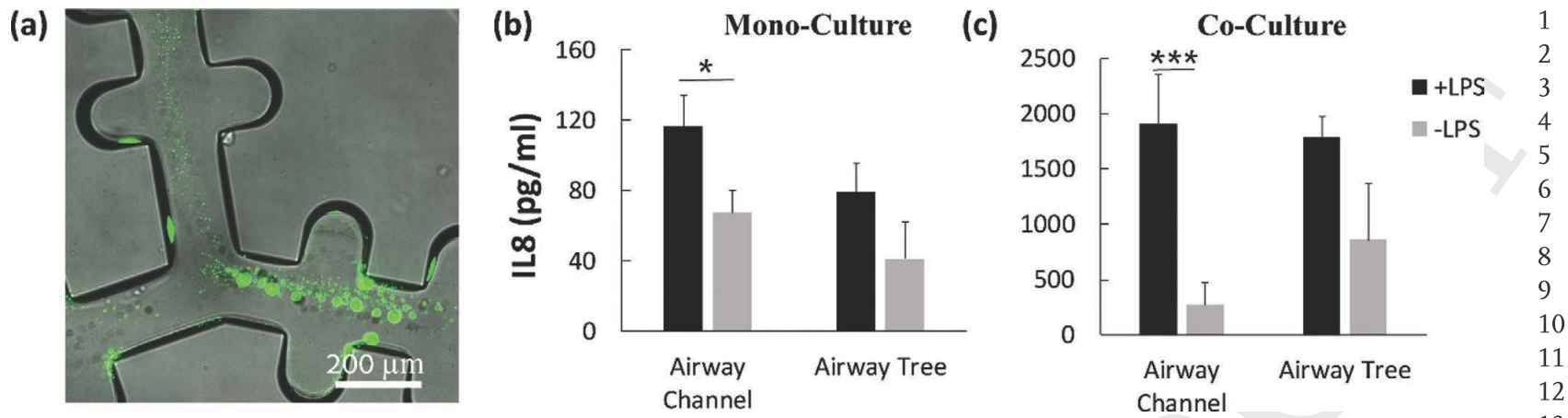

Figure 4. Mimicking bacterial inflammation in the acini-on-chip. a) Qualitative snapshot of a local deposition field after 2 min exposure with a commercial nebulizer: dry channel on a glass slide, FluNa 2.5 µg mL^{-1} in PBS. b,c) Plots show the secretion of IL8 cytokines following 48 h poststimulation with LPS nebulization (10 µg mL^{-1}) or PBS nebulization as a control, measured by enzyme-linked immunosorbent assay (ELISA): (b) monoculture (hAELVi) and (c) coculture (hAELVi and THP-1). Cells were grown until a full confluent monolayer was achieved (14–35 days). Data shown as mean ± SD (airway channel: mono- $n = 3$, coculture $n = 6$, alveolated airway tree: mono- and coculture $n = 3$ independent experiments); $^{***}p < 0.001$, (ANOVA). $^{*}p < 0.05$, compared with controls (i.e., cells cultured without LPS).

expected from the coculture, the THP-1 augments IL-8 secretion by more than an order of magnitude, thus demonstrating the important role played by THP-1 in recapitulating realistic immune functions within the acini-on-chip. The influence of the LPS exposure on the epithelial integrity was examined by staining of the tight junction proteins, i.e., ZO-1 and Occludin, 72 h after the LPS exposure, with no change in the epithelial monolayer integrity (not shown for brevity); a result consistent with previous findings.[38]

3. Conclusions

The acini-on-chips presently described are the first in vitro platforms, to the best of our knowledge, that integrate characteristic airflows of the respiratory zone within a morphologically relevant anatomy while guaranteeing underlying epithelial barrier characteristics. To date, all efforts within lung-on-chip platforms have been performed in straight channels. For the first time, we have expanded such concept to complex airway tree networks mimicking more closely native acinar airway anatomies. Using a novel cell model system (hAELVi), we have successfully reconstructed relevant cell populations of the alveolar region and demonstrated the establishment of a functional epithelial barrier in an anatomically relevant manner. We used two complementary techniques to demonstrate a functional barrier in a coculture system where macrophage-like cells are grown on top of the epithelial cell layer: staining of tight junction proteins as well as permeability assays. Within the scope of establishing an in vitro acinar benchmark, THP-1 cells have been used to mimic alveolar macrophages and deliver valuable insight that can be developed in the future into a biosystem consisting of lung primary cells. We successfully demonstrated a long-term cell culture inside the lung-on-chip while maintaining functional barrier properties. The presented assays were performed following up to 35 days from seeding, providing a promising platform for both acute (normally, 48–72 h) and subacute (14–28 days) toxicity assays in the deep alveolar regions. As a proof-of-concept, the devices were leveraged to mimic the onset of bacterial infection. Following a realistic aerosol exposure scenario with inhaled airborne droplets in airflow, LPS was introduced into the devices and cell response was measured by IL8 secretion. Our in vitro biosystem was able to recapitulate the protective responses from the epithelium and its further enhancement by the immune cells. Possible directions include integrating additional cell types that play a critical role in the orchestra of the immune response, such as endothelia and neutrophils. Here, we have used the hAELVi cells with a unique opportunity to help bridge between in vivo and in vitro studies in respiratory research. With the practical difficulty in obtaining human alveolar primary cells and alveolar macrophages, the variability between different donors can mask effects and jeopardize delivering clear conclusions. As such, the hAELVi and THP-1 cells provide an attractive alternative in establishing a novel in vitro benchmark for other researchers and scientists to compare with (e.g., control), allowing for example to "normalize" differences between different donors. Such biological functionality in conjunction with mimicking more closely morphological constraints (i.e., airway anatomy) and physiological conditions (e.g., respiratory airflows) offer tangible opportunities for drug toxicity screens and aerosol deposition assays amongst other.

4. Experimental Section

Microdevice Fabrication: Standard soft-lithography techniques were adopted for microfabrication of PDMS-based microfluidic devices;[51] such techniques were combined with a modified method for master production using deep reactive ion etching of a silicon on insulator[10] wafer to manufacture delicate features of the acinar model.

A clean 2 in. wafer was dehydrated on a hot plate (300 °C, 5 min). SU-8 2150 photoresist (Microchem) was spin-coated on the wafer at 500 rpm for 10 s using a 100 rpm s^{-1} acceleration rate, then 3000 rpm for 30 s with acceleration of 300 rpm s^{-1}. The wafer was kept overnight on a leveled surface in a sealed petri dish to improve surface flatness, then baked on a hot plate (65 °C 5 min, 90 °C 30 min), and exposed to UV light through a photomask at a total dose of 400 mJ cm^{-2} using an MA6 mask aligner (Karl Suss). Postexposure bake was performed on a hot plate (65 °C 5 min, 95 °C 13 min) and then the substrate was

developed in propylene glycol monomethyl ether acetate, rinsed with isopropyl alcohol, and spin dried. The resulting SU-8 pattern on the silicon wafer is then continuously used as a master template for PDMS casting, and manufacture of PDMS microdevices. PDMS was mixed with a curing agent (DOWSIL 184 Silicon Elastomer Kit) at a 10:1 volume ratio, poured on the template, and baked for 60 min at ≈65 °C. Cured PDMS was pealed from the wafer, punched using a 1 mm biopsy punch (Miltex, 3331) to create inlets and outlets, and rinsed with 70% ethanol. The PET membrane with 0.4 µm pore size (Corning), was irreversibly bonded to the acinar microchannels using a "stamping" technique.[52] Briefly, liquid PDMS (10:1) was spin-coated on a glass side (500 rpm for 20 s acceleration 100 rpm s^{-1}, 4000 rpm for 20 min acceleration 127 rpm s^{-1}.), creating a thin liquid layer. Thereafter, a readily made PDMS microdevice was gently brought into contact with the thin layer (for 30 s) and immediately attached to the PET membrane from one side. The structure was cured at 65 °C for an hour to accomplish a complete bonding, and placed using stamping on top of a PDMS well to be further filled with culture media. Finally, a glass cover slip (Corning) was prepared and cleaned with ethanol and bonded to the bottom side (reservoir) of the device.

Cell Culture: hAELVi cells (InSCREENeX, INS-CI-1015) were cultured as previously described.[23] In brief, hAELVi cells were cultured in small airway epithelial cell growth medium (SAGM) BulletKit (Lonza CC-3118) supplemented with 1% FBS and 1% penicillin/streptomycin (P/S) (Life Technologies, 15140-122). Prior to seeding, flasks were coated with coating buffer (1% (v/v) fibronectin; (Corning, 33016015) and 1% (v/v) collagen (Sigma, C4243)). The medium was changed every two to three days. When cells reached 90% confluency, they were trypsinized and used for maintenance or experiments, as described below.

The THP1 cells were cultured in RPMI-1640 (Biological Industries Israel Beit-Haemek Ltd. 01-100-1A) supplemented with 10% FBS and 1% penicillin–streptomycin (P/S). THP-1 monocytes (ATCC, TIB-202) were differentiated to macrophage-like cells using 7.5 ng mL^{-1} of phorbol 12-myri-state 13-acetate (PMA; Sigma, P8139) following incubation of 16 h. Differentiated THP-1 cells were trypsinized and used in the experiments.

All cells were grown under 37 °C, 5% CO_2, and 95% humidity.

Mycoplasma controls were performed routinely and never showed infection.

Insert Cell Culture: hAELVi cells (2×10^5 cells cm^{-2}) were seeded on coated Transwell polyester membranes (Corning 3460; growth area 1.12 cm^2; pore size 0.4 µm). Under liquid–liquid conditions, 500 µL of medium was perfused in the apical side and 1.5 mL at the basolateral. The medium was changed every second day. For air–liquid conditions (ALI), at 2 days postseeding, the medium from the apical compartment was aspirated and the cells were further fed from the basolateral compartment with 500 µL of medium.

Microfluidic Cell Culture: The devices were sterilized following three rounds of UV (254 nm), 15 min each. Following sterilization, the apical side was incubated with coating buffer for 1 h in 37 °C, 5% CO_2, and 95% humidity. All devices were washed with PBS and seeded with cells without drying the membrane.

Monocultures: 10 µL or 5 µL of a hAELVi cell suspension (3×10^7 cells mL^{-1}), were seeded on the membrane of a coated full tree or the airway channel, respectively. Both the basolateral and apical compartments were filled with medium. Following 48 h in liquid–liquid conditions the medium from the apical compartment was aspirated, allowing the cells to grow at the ALI. The cells were further fed every second day from the basolateral compartment, by withdrawing the liquid from the basolateral side and then injecting fresh medium changed the medium.

Cocultures: hAELVi monocultures pregrown for 20–35 days were used to set up the coculture with THP-1 cells. Differentiated THP-1 cells (1×10^7 cells mL^{-1}), 10 or 5 µL of the suspended cells were seeded on top of hAELVi cells in the full tree or the airway channel, respectively. In the basolateral compartment, SAGM was applied. The coculture was cultivated between 1 and 7 days at 37 °C, 5% CO_2.

Scanning Electron Microscopy: The samples were washed three times with PBS and fixed in primary fixative buffer (1% paraformaldehyde (PFA) and 2% GA in 0.1 M NaP pH 7.4 and 3% sucrose) for 60 min at RT. Following three washes with 0.1 M cacodylate buffer, pH 7.4 the samples postfixed with 1% osmium tetraoxide in 0.1 M cacodylate buffer for 15 min at RT. Next, the samples dehydrated through a graded ethanol series, processed by critical point drying and sputter coated with chromium (5 nm). Images were taken with a Zeiss ULTRA plus field-emission scanning electron microscope.

Immunostaining: hAELVi and differentiated THP-1 cells were washed with PBS, fixed with 3.6% PFA (Sigma-Aldrich, 47608) in PBS for 15 min at RT, following a rinse with PBS. Next, the cells were permeabilized with 0.5% Triton X-100 (Sigma-Aldrich, T8787) in PBS for 5 min at RT. The cells were washed with PBS and blocked with 10% serum in PBS for 1 h. For DAPI nucleic acid staining cells were incubated with DAPI solution (ThermoFisher Scientific, D1306), diluted with PBS (ratio of 1:1000) for 5 min at RT. For tight junction proteins, Zonula occludens-1 (ZO-1) and Occludin staining, cells were incubated with the primary antibodies rabbit anti-ZO1 (ThermoFisher Scientific, 617300)/mouse antioccludin (ThermoFisher scientific, 331500) diluted with PBS (ratio of 1:200) overnight at 4 °C, followed by incubation with secondary antibody Alexa Fluor 488 antirabbit/antimouse (Jackson ImmunoResearch, 111-545-144/115-545-062), diluted with PBS (ratio of 1:400) for 1 h at RT. The differentiation of THP-1 toward macrophage-like cells was examined with FITC antihuman CD11b (BioLegend, 301329), diluted with PBS (ratio of 1:20) for 1 h at RT. Confocal microscopy imaging of fluorescent immunostaining was performed (Nikon Eclipse Ti with spinning disk, Yokogawa, Japan).

Transport Studies: The devices were seeded with mono- or coculture as previously described. The cells were allowed to grow for 14–25 days (in ALI from day 2). Transport experiments were then performed according to Elbert et al.[22] Briefly, the cells were washed twice with prewarmed Krebs–Ringer buffer (KRB; NaCl 142.03×10^{-3} M, KCl 2.95×10^{-3} M, $K_2HPO_4{}^*3H_2O$ 1.49×10^{-3} M, HEPES 10.07×10^{-3} M, D-glucose 4.00×10^{-3} M, $MgCl_2{}^*6H_2O$ 1.18×10^{-3} M, $CaCl_2{}^*2H_2O$ 4.22×10^{-3} M; pH 7.4), and incubated in KRB for 45 min. Next, medium was aspirated and 10 µL FluNa (10 µg mL^{-1} in KRB) were added to the apical compartment and 500 KRB were added to the basolateral compartment. The devices were placed in the incubator and 30 µL samples were taken every 30 min, from the basolateral compartment only, and transferred into a 384-well plate to measure FluNa concentrations. Sampled volumes were refilled with 30 µL KRB. The samples in the 384-well plates were measured with a Varioskan LUX plate reader using wavelengths of 495 nm (em) and 520 nm (ex).

TEER Measurement: The TEER was measured as previously described.[23] Briefly, 100 000 cells cm^{-2} cells were seeded on precoated PET membrane with a pore size of 0.4 µm and a growth area of 0.33 cm^2 (Corning, CLS3460). 48 h after seeding the medium from the apical side was aspirated to allow ALI. Before measuring TEER, the apical side was refilled with 300 µL prewarmed medium and the basolateral compartments were filled up to a final volume of 500 µL. Following 1 h of incubation, the TEER was measured in all samples using an epithelial volt-ohm meter (Millicell ERS-2) equipped with chopstick electrodes (MERSSTX01, Millicell). The electrical resistance was calculated by subtracting the value of blank inserts containing medium from all samples, and multiplication with the cultivation area of the inserts (0.33 cm^2).

LPS Stimulations: The exposure assay was conducted using a Mini Compressor Nebulizer (Bio-rich). The nebulizer plastic parts were rinsed with soap (Ariel Clean liquid soap) followed by ethanol, and then sterilized for 15 min under UV radiation (254 nm). The nebulizer cup was loaded with PBS or LPS diluted with PBS (10 µg mL^{-1}) (L4516 SIGMA). Using an adaptor, the outlet of the nebulizer cup was connected to the apical compartment of the acini-on-chip devices using Cole–Parmer tubing (cat # 06400–90). Each exposure assay was conducted for up to 4 min.

IL8 Secretion Assay: Cell culture supernatants were assayed using ELISA for IL-8 (Termo fisher scientific) following the manufacturer's instructions.

Statistical Analysis: Data are representative of 3–9 independent experiments and shown as mean ± SD. Two-way ANOVA was performed using GraphPad Prism 8 software (GraphPad).

Supporting Information

Supporting Information is available from the Wiley Online Library or from the author.

Acknowledgements

The authors thank Prof. Netanel Korin (Technion) and Dr. Enas Abu-Shah (Oxford University, UK) for helpful discussions. The authors thank Dr. Shaulov from the Biomedical Core Facilities (Technion) for technical support with the electron microscopy. This work was supported by the German Israel Foundation (GIF, Grant Agreement No. I-1348-409.10/2016) and the European Research Council (ERC) under the European Union's Horizon 2020 research and innovation program (Grant Agreement No. 677772). Microfabrication was conducted at the Micro-Nano Fabrication & Printing Unit (MNF & PU) of the Technion and supported by the Russel Berrie Nanotechnology Institute (RBNI, Technion).

Conflict of Interest

The authors declare no conflict of interest.

Keywords

epithelial barrier, in vitro assays, microfluidics, organ-on-chip, pulmonary infection

Received: February 26, 2019
Revised: June 30, 2019
Published online:

[1] T. C. J. Mertens, H. Karmouty-Quintana, C. Taube, P. S. Hiemstra, *Pulm. Pharmacol. Ther.* **2017**, *45*, 101.
[2] J. Seok, H. S. Warren, A. G. Cuenca, M. N. Mindrinos, H. V. Baker, W. Xu, D. R. Richards, G. P. McDonald-Smith, H. Gao, L. Hennessy, C. C. Finnerty, C. M. López, S. Honari, E. E. Moore, J. P. Minei, J. Cuschieri, P. E. Bankey, J. L. Johnson, J. Sperry, A. B. Nathens, T. R. Billiar, M. A. West, M. G. Jeschke, M. B. Klein, R. L. Gamelli, N. S. Gibran, B. H. Brownstein, C. Miller-Graziano, S. E. Calvano, P. H. Mason et al. *Proc. Natl. Acad. Sci. USA* **2013**, *110*, 3507.
[3] C. H. Wong, K. W. Siah, A. W. Lo, *Biostatistics* ~~2018~~, *20*, 273.
[4] J. Rice, *Nature* **2012**, *484*, ~~309~~.
[5] P. S. Hiemstra, G. Grootaers, A. M. van der Does, C. A. M. Krul, I. M. Kooter, *Toxicol. Vitr.* **2018**, *47*, 137.
[6] J. Tenenbaum-Katan, A. Artzy-Schnirman, R. Fishler, N. Korin, J. Sznitman, *Biomicrofluidics* **2018**, *12*, 042209.
[7] A. O. Stucki, J. D. Stucki, S. R. R. Hall, M. Felder, Y. Mermoud, R. A. Schmid, T. Geiser, O. T. Guenat, *Lab Chip* **2015**, *15*, 1302.
[8] D. Huh, B. D. Matthews, A. Mammoto, M. Montoya-Zavala, H. Y. Hsin, D. E. Ingber, *Science* **2010**, *328*, 1662.
[9] N. J. Douville, P. Zamankhan, Y.-C. Tung, R. Li, B. L. Vaughan, C.-F. Tai, J. White, P. J. Christensen, J. B. Grotberg, S. Takayama, *Lab Chip* **2011**, *11*, 609.
[10] R. Fishler, P. Hofemeier, Y. Etzion, Y. Dubowski, J. Sznitman, *Sci. Rep.* **2015**, *5*, 14071.
[11] D. Huh, D. C. Leslie, B. D. Matthews, J. P. Fraser, S. Jurek, G. A. Hamilton, K. S. Thorneloe, M. A. McAlexander, D. E. Ingber, *Sci. Transl. Med.* **2012**, *4*, 159ra147.
[12] K. H. Benam, R. Novak, J. Nawroth, M. Hirano-Kobayashi, T. C. Ferrante, Y. Choe, R. Prantil-Baun, J. C. Weaver, A. Bahinski, K. K. Parker, D. E. Ingber, *Cell Syst.* **2016**, *3*, 456.
[13] A. Jain, R. Barrile, A. D. van der Meer, A. Mammoto, T. Mammoto, K. De Ceunynck, O. Aisiku, M. A. Otieno, C. S. Louden, G. A. Hamilton, R. Flaumenhaft, D. E. Ingber, *Clin. Pharmacol. Ther.* **2018**, *103*, 332.
[14] C. Blume, R. Reale, M. Held, T. M. Millar, J. E. Collins, D. E. Davies, H. Morgan, E. J. Swindle, *PLoS One* **2015**, *10*, e0139872.
[15] J. Sznitman, *J. Biomech.* **2013**, *46*, 284.
[16] F. Blank, B. M. Rothen-Rutishauser, S. Schurch, P. Gehr, *J. Aerosol Med.* **2006**, *19*, 392.
[17] A. G. Lenz, T. Stoeger, D. Cei, M. Schmidmeir, N. Semren, G. Burgstaller, B. Lentner, O. Eickelberg, S. Meiners, O. Schmid, *Am. J. Respir. Cell Mol. Biol.* **2014**, *51*, 526.
[18] M. Röhm, S. Carle, F. Maigler, J. Flamm, V. Kramer, C. Mavoungou, O. Schmid, K. Schindowski, *Int. J. Pharm.* **2017**, *532*, 537.
[19] M. H. Wong, M. D. Johnson, *PLoS One* **2013**, *8*, e55545.
[20] A. J. Byrne, S. A. Mathie, L. G. Gregory, C. M. Lloyd, *Thorax* **2015**, *70*, ~~207020~~.
[21] N. Daum, A. Kuehn, S. Hein, U. F. Schaefer, H. Huwer, C. Lehr, *Methods Mol. Biol.* **2012**, *806*, 31.
[22] K. J. Elbert, U. F. Schäfer, H. J. Schäfers, K. J. Kim, V. H. Lee, C. M. Lehr, *Pharm. Res.* **1999**, *16*, 601.
[23] A. Kuehn, S. Kletting, C. de Souza Carvalho-Wodarz, U. Repnik, G. Griffiths, U. Fischer, E. Meese, H. Huwer, D. Wirth, T. May, N. Schneider-Daum, C. M. Lehr, *ALTEX* **2016**, *33*, 251.
[24] W. Chanput, J. J. Mes, H. J. Wichers, *Int. Immunopharmacol.* **2014**, *23*, 37.
[25] C. Schulz, X. Lai, W. Bertrams, A. L. Jung, A. Sittka-Stark, C. E. Herkt, H. Janga, K. Zscheppang, C. Stielow, L. Schulte, S. Hippenstiel, J. Vera, B. Schmeck, *Sci. Rep.* **2017**, *7*, 11988.
[26] C. Alexander, E. T. Rietschel, *J. Endotoxin Res.* **2001**, *7*, 167.
[27] A. A. Hislop, J. S. Wigglesworth, S. R. Desai, *Early Hum. Dev.* **1986**, *13*, 1.
[28] M. G. Ménache, W. Hofmann, B. Asgharian, F. J. Miller, *Inhalation Toxicol.* **2008**, *20*, 101.
[29] J. Stocks, P. H. Quanjer, *Eur. Respir. J.* **1995**, *8*, 492.
[30] J. Tenenbaum-Katan, R. Fishler, B. Rothen-Rutishauser, J. Sznitman, *Biomicrofluidics* **2015**, *9*, 014120.
[31] A. Tsuda, F. S. Henry, J. P. Butler, *J. Appl. Physiol.* **1995**, *79*, 1055.
[32] M. Humayun, C. W. Chow, E. W. K. Young, *Lab Chip* **2018**, *18*, 1298.
[33] R. Bhowmick, H. Gappa-Fahlenkamp, *Lung* **2016**, *194*, 419.
[34] K. A. Foster, C. G. Oster, M. M. Mayer, M. L. Avery, K. L. Audus, *Exp. Cell Res.* **1998**, *243*, 359.
[35] D. Konar, M. Devarasetty, D. V. Yildiz, A. Atala, S. V. Murphy, *Biomed. Eng. Comput. Biol.* **2016**, *2016*, 17.
[36] B. Zhang, M. Radisic, *Lab Chip* **2017**, *17*, 2395.
[37] D. E. Ingber, *Cell* **2016**, *164*, 1105.
[38] K. H. Benam, R. Villenave, C. Lucchesi, A. Varone, C. Hubeau, H. H. Lee, S. E. Alves, M. Salmon, T. C. Ferrante, J. C. Weaver, A. Bahinski, G. A. Hamilton, D. E. Ingber, *Nat. Methods* **2016**, *13*, 151.
[39] C.-M. Lehr, *Cell Culture Models of Biological Barriers: In Vitro Test Systems for Drug Absorption and Delivery*, CRC Press, ~~Boca Raton~~, ~~FL~~ ~~2003~~.
[40] S. Kletting, S. Barthold, U. Repnik, G. Griffiths, B. Loretz, N. Schneider-Daum, C. deS. Carvalho-Wodarz, C. M. Lehr, *ALTEX – Altern. Anim. Exp.* **2018**, *35*, 211.
[41] O. Y. F. Henry, R. Villenave, M. J. Cronce, W. D. Leineweber, M. A. Benz, D. E. Ingber, *Lab Chip* **2017**, *17*, 2264.
[42] Y. B. Arlk, M. W. Van Der Helm, M. Odijk, L. I. Segerink, R. Passier, A. Van Den Berg, A. D. Van Der Meer, *Biomicrofluidics* **2018**, *12*, 042218.
[43] F. Liu, W. Li, J. Pauluhn, H. Trübel, C. Wang, *Toxicology* **2013**, *304*, 158.

[44] A. K. Mayer, M. Muehmer, J. Mages, K. Gueinzius, C. Hess, K. Heeg, R. Bals, R. Lang, A. H. Dalpke, *J. Immunol.* **2007**, *178*, 3134.
[45] B. L. Laube, *Respir. Care* **2005**, *50*, 1161.
[46] B. L. Laube, *Transl. Respir. Med.* **2014**, *2*, 1.
[47] W. F. Tonnis, G. F. Kersten, H. W. Frijlink, W. L. J. Hinrichs, A. H. de Boer, J.-P. Amorij, *J. Aerosol Med. Pulm. Drug Delivery* **2012**, *25*, 249.
[48] C. A. Fromen, G. R. Robbins, T. W. Shen, M. P. Kai, J. P. Y. Ting, J. M. DeSimone, *Proc. Natl. Acad. Sci. USA* **2015**, *112*, 488.
[49] L. D. Mastrandrea, *Vasc. Health Risk Manag.* **2010**, ~~*2010*~~, 47.
[50] S. B. Fiel, *Expert Rev. Respir. Med.* **2008**, *2*, 479.
[51] D. C. Duffy, J. C. McDonald, O. J. A. Schueller, G. M. Whitesides, *Anal. Chem.* **1998**, *70*, 4974.
[52] B. Chueh, D. Huh, C. R. Kyrtsos, T. Houssin, N. Futai, S. Takayama, *Anal. Chem.* **2007**, *79*, 3504.

ADVANCED BIOSYSTEMS

Reprint Order Form

Please complete this form and return it via E-Mail to the Editorial Office at

E-mail: adv-biosys@wiley-vch.de

Wiley-VCH Verlag GmbH & Co. KGaA
Advanced Biosystems
Boschstr. 12
69469 Weinheim
Germany

Manuscript No.: _____
Customer No.: (if available) _____
Purchase Order No.: _____
Author: _____
Date: _____

Charges for Reprints in Euro (excl. VAT), prices are subject to change. Minimum order 50 copies; single issues for authors at a reduced price.

No. of pages	50 copies	100 copies	150 copies	200 copies	300 copies	500 copies
1–4	345,—	395,—	425,—	445,—	548,—	752,—
5–8	490,—	573,—	608,—	636,—	784,—	1077,—
9–12	640,—	739,—	786,—	824,—	1016,—	1396,—
13–16	780,—	900,—	958,—	1004,—	1237,—	1701,—
17–20	930,—	1070,—	1138,—	1196,—	1489,—	2022,—
every additional 4 pages	147,—	169,—	175,—	188,—	231,—	315,—

Information regarding VAT: Please note that from German sales tax point of view, the charge for Reprints, Issues or Posters is considered as "supply of goods" and therefore, in general, such delivery is a subject to German sales tax. However, this regulation has no impact on customers located outside of the European Union. Deliveries to customers outside the Community are automatically tax-exempt. Deliveries within the Community to institutional customers outside of Germany are exempted from the German tax (VAT) only if the customer provides the supplier with his/her VAT number. The VAT number (value added tax identification number) is a tax registration number used in the countries of the European Union to identify corporate entities doing business there. Starting with a country code (e.g. FR for France), followed by numbers.

Please send me and bill me for

☐ no. of reprints
- ☐ airmail (+ 25 Euro)
- ☐ surface mail
- ☐ Fedex No.:_____

☐ no. of issue (1 copy: 54 Euro)
- ☐ airmail (+ 25 Euro)
- ☐ surface mail
- ☐ Fedex No.:_____

☐ high-resolution PDF file (330 Euro)
E-mail address: _____

☐ Special Offer:

If you order 200 or more reprints you will get a PDF file for half price.

Please note: It is not permitted to present the PDF file on the internet or on company homepages.

Cover Posters (prices excl. VAT)
Posters of published covers are available in two sizes:

☐ DIN A2 42 x 60 cm / 17 x 24in (one copy: 39 Euro)

☐ DIN A1 60 x 84 cm / 24 x 33in (one copy: 49 Euro)

Postage for shipping posters overseas by airmail:
+ 25 Euro
Postage for shipping posters within Europe by surface mail: + 15 Euro

_____
Date, Signature

VAT number: _____

Mail reprints / copies of the issue to:

_____
_____
_____
_____
_____

Send bill to:

_____
_____
_____
_____

☐ **I will pay by bank transfer**

☐ **I will pay by credit card**

VISA, Mastercard and AMERICAN EXPRESS

For your security please use this link (Credit Card Token Generator) to create a secure code Credit Card Token and include this number in the form instead of the credit card data. Click here:
https://www.wiley-vch.de/editorial_production/index.php

						V								

CREDIT CARD TOKEN NUMBER

Wiley-VCH Verlag GmbH & Co. KGaA – A company of John Wiley & Sons, Inc. -
Location of the Company: Weinheim - Trade Register: Mannheim, HRB 432833.
Chairman of the Supervisory Board: Stephen Michael Smith.
General Partner: John Wiley & Sons GmbH, Location: Weinheim –
Trade Register Mannheim, HRB 432296 – Managing Director: Sabine Steinbach und Guido Herrmann

WILEY-VCH